Journal of Sound and Vibration 430 (2018) 174–184

Contents lists available at ScienceDirect

Journal of Sound and Vibration

journal homepage: www.elsevier.com/locate/jsvi

A resonant beam damper tailored with Acoustic Black Hole features for broadband vibration reduction

Tong Zhou, Li Cheng*

Department of Mechanical Engineering, The Hong Kong Polytechnic University, Hong Kong

ARTICLE INFO

Article history:
Received 12 February 2018
Received in revised form 24 May 2018
Accepted 30 May 2018

Handling Editor: J. Macdonald

Keywords:
Acoustic black hole
Dynamic vibration absorber
Resonant beam damper
Waveguide absorber

ABSTRACT

By capitalizing on the Acoustic Black Hole (ABH) phenomenon, a so-called ABH-featured Resonant Beam Damper (ABH-RBD) is proposed for the broadband vibration suppressions of a primary structure. As an add-on device to be attached to the primary structure, the proposed ABH-RBD embraces the principles of both dynamic vibration absorbers and waveguide absorbers. Its design and implementation do not need a tedious parameter tuning, thus showing robustness to accommodate structural variations in the primary structure. Using a beam as a benchmark, both numerical simulations and experiments show that multiple resonances of the primary structure can be significantly reduced by the proposed ABH-RBD, and the same ABH-RBD is effective on different primary systems. Typical control effects and the underlying mechanisms are investigated. Analyses reveal the existence of three types of vibration reduction mechanisms, manifested differently and dominated by different physical process, *i.e.* structural interaction, damping enhancement and their combination. Comparisons with a conventional uniform beam absorber show that the superiority of the proposed ABH-RBD is attributed to its ABH-specific features exemplified by the enriched system dynamics and the enhanced broadband damping.

1. Introduction

The use of add-on vibration reduction devices is a common method to suppress undesirable vibrations of a structure [1]. A dynamic vibration absorber (DVA) is one of such devices which are most commonly used. A DVA is tuned for neutralizing vibratory energy through its interaction with the host structure. The basic form of a DVA contains a mass component connected by spring and damping elements to the vibrating structure called primary structure [2]. Through a precise tuning of the DVA parameters, the vibration response of the primary structure can be significantly reduced at the tuning frequency owing to its strong interaction with the DVA. Damping helps extend the working frequency band of the DVA at the expenses of compromising the control performance at the tuning frequency [3]. To achieve the maximum vibration attenuation within the targeted frequency band, both the frequency and the damping of the absorber have to be meticulously tuned and optimized [4]. Apart from its basic configuration, various designs of DVAs have been attempted and reported in the literature, as reviewed in Ref. [5]. A resonant beam damper (RBD) is one type of continuous DVAs. As shown in Fig. 1(a), the fundamental bending mode of a cantilever absorber is utilized to generate the interaction with the primary system [6,7]. To broaden the working bandwidth around the targeted frequency, multi-layered beam-type neutralizers, composed of several stacked

* Corresponding author.
E-mail address: li.cheng@polyu.edu.hk (L. Cheng).

https://doi.org/10.1016/j.jsv.2018.05.047
0022-460X/

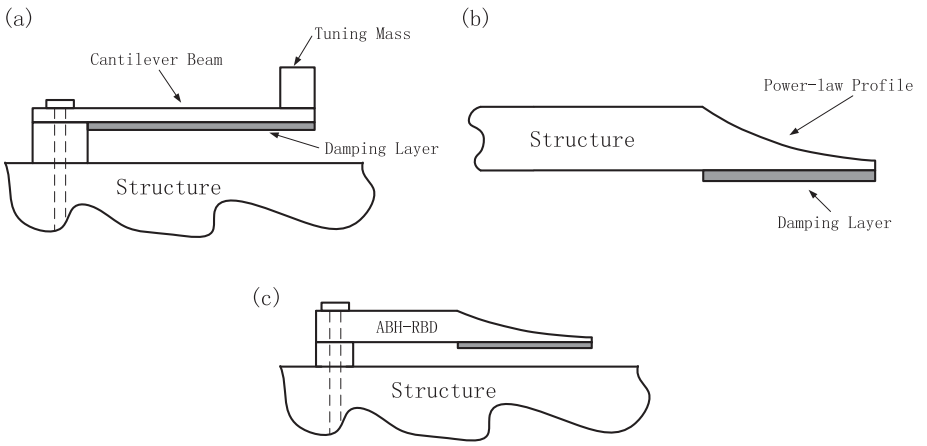

Fig. 1. (a) Resonant Beam Damper, (b) ABH tapered beam (c) ABH-RBD.

beams with slightly different lengths, were proposed [8]. Several types of multi-degree-of-freedom (DOF) DVAs have also been studied, whose parameters need to be tuned to each structural resonance so that multiple resonant peaks of the primary structure can be controlled in a wide frequency range [9,10]. Towards the same objective of controlling broadband resonant peaks, multiple 1-DOF DVAs have also been attempted on beams [11–13] or plates [14,15], with each absorber dealing with a particular structural resonance. However, the tuning procedure of the entire absorber system in this case becomes quite complicated and tedious since the whole cluster of DVAs needs to be tuned simultaneously due to their mutual interactions [11,15].

Alternatively, a waveguide absorber (WGA) is another type of add-on devices for vibration control. Taking different forms based on beam or plate elements, a WGA makes use of the waveguide phenomenon to draw the vibratory energy away from the primary system. With a proper damping treatment and sufficient wave propagating distance, the reflection of the extracted vibrational energy back to the primary system can be limited, and in the ideal case, the WGA behaves like an infinite or boundless energy sinker [1,16]. Due to the relatively weak dynamic coupling between the WGA and the primary system, the WGA needs to be properly designed to provide sufficient energy dissipation to achieve multi-resonance attenuations. To ensure the maximum increase in the added loss factor to the primary system, the mechanical impedance of the WGA and that of the primary structure at the attachment point should be matched to satisfy the impedance-matching condition [16]. Meanwhile, it is shown that both the attachment locations and the number of absorbers to be used are important for generating sufficient control effects [17–19]. Efforts have also been made to reduce the dimension and the occupation space of the absorbers through various structural designs [20,21]. Despite the existing efforts, the design of more versatile and efficient WGAs is still needed to cope with practical applications.

Despite their widespread use, both DVAs and WGAs pose problems for broadband vibration reductions in terms of design and implementations. For the former, the physical parameters of the DVA cluster need to be meticulously tuned, which is a quite tedious and complex process. In addition, structural or operational changes in the primary structure may jeopardize the effectiveness of the designed DVAs. For the latter, conventional structural elements can hardly provide the required energy dissipations unless multiple absorbers with large structural dimensions and massive damping materials are used. Meanwhile, variations of environmental factors like the temperature can also easily change the properties of the damping materials, thus influencing the effectiveness of the designed WGAs.

To tackle these problems, the present study proposes a new add-on device by capitalizing on a combined DVA and WGA principle through the exploitation of the unique features of the so-called 'Acoustic Black Hole' (ABH) phenomenon. The targeted outcome is a compact and light weighted vibration reduction device to achieve the broadband vibration suppressions without a complex tuning procedure. Meanwhile, it should be robust enough to accommodate structural and operational variations in the primary vibrating system.

Studies on ABH have been drawing an increasing attention in the vibration community during the last two decades. In the one-dimensional case, an ABH wedge (Fig. 1(b)) is tailored to have a thickness variation according to a power function, $h(x) = \varepsilon x^m, m \geq 2$, in which x is the taper length coordinate. When flexural waves travel towards the tip of the taper, their phase and the group velocities gradually reduce and the wave amplitude increase progressively. If the thickness of the taper goes to zero, the bending waves will take an infinitely long time to travel inside the tapered area, resulting in zero wave reflections [22]. In practice, however, the wedge thickness can never reach zero. When this happens, the inevitable wave reflections caused by the truncated tip can be countered by covering the taper with damping materials [23]. Owing to the high energy density within the tip region as a result of the wave compression and focalization, a small amount of damping materials turns out to be enough to create a significant damping increase in the entire taper. Typical features of ABH structures have been extensively studied and revealed by previous work. Apart from the aforementioned wave trapping phenomenon, the energy shift

from the uniform portion of a structure towards the tapered ABH portion has been demonstrated, alongside the rich distributed local resonant modes with high modal loss factors [24–26]. Studies also showed that the use of an additional platform (by extending the truncated tip with a constant thickness) leads to an appreciable enhancement of the ABH effects [26,27]. For practical implementations, various ABH designs such as spiral ABH configurations [28] have also been proposed to reduce the space occupation. Up to now, research has been limited to the study of elementary ABH elements embedded in beams [29–31] and plates [32–34], instead of as an add-on anti-vibration device. Although embedding ABH elements into a primary structure is shown to bring about beneficial dynamic effects, the design is intrusive to the structure and the thin thickness in the taper or indentation area significantly reduces the structural stiffness, thus jeopardizing its load-bearing capability and other mechanical properties [26].

In the present paper, we propose and investigate a resonant beam damper (RBD) configuration by embracing the ABH principle, referred to as 'ABH-RBD' (Fig. 1(c)) for the suppressions of broadband resonant peaks of a host structure, exemplified by a beam. Different from the embedding philosophy in the primary vibratory system, as described before, the proposed ABH-RBD is to be used as a separable add-on device or auxiliary system mounted on the original host structure.

The outline of the paper is as follows. The proposed ABH-RDB is first described, followed by a description of the simulation model and numerical analysis method. Although the proposed ABH-RDB is not limited to one particular type of primary structures, a beam is selected as a benchmark case for the sake of simplicity. The vibration suppression ability of the proposed ABH-RDB is then demonstrated. Observed typical peak reductions on the frequency response function curves are analyzed to explain different vibration control mechanisms involved. The vibration reductions owing to the structural interactions and energy dissipations are analyzed systematically through varying the parameters of the coating absorbing layer in the tapered portion of the auxiliary ABH-RBD. Comparisons with a uniform add-on beam with the same weight and damping treatment are performed to show the critical roles played by the ABH features. Experiments are then conducted to verify the broadband vibration suppression phenomena as well as the typical vibration control effects predicted in numerical simulations.

2. Primary structure with ABH-RBD and simulation model

As shown Fig. 2, the configuration under investigation contains a primary host structure (a uniform beam) and an auxiliary ABH-RBD connected by a small connector. The length (denoted by L) and the thickness of the host uniform beam are 300 mm and 8 mm, respectively. The ABH-RBD can be further divided into two sub-sections: a tapered portion with an ABH thickness profile and a uniform portion. The uniform region of the ABH-RBD is 1/6 L long and 3 mm thick. The tapered portion has the same length as the uniform portion and the thickness varies from 3 mm to 0.1 mm following a parabolic variation law ($h(x) = \varepsilon x^2 + h_0$, where ε is a constant). A viscoelastic damping layer with a constant thickness ($h_d = 1$mm) is coated over the surface of the entire tapered region. The total weight and the total length of the ABH-RBD is 9.2% and 1/3 of that of the primary system, respectively. A small connector with a dimension of 8 × 1 mm is located at 60%·L from the left end of the host beam and mounted over the surface of the primary system. The width of all elements is set to be the same (20 mm). The coating material on the ABH taper is a viscoelastic tape, 3M™ F9473P [35], with a constant Young's modulus and loss factor η_d adopted in simultations. The rest of the system is set to be aluminium (detailed material parameters tabulated in Table 1).

Finite element (FE) simulations were conducted using COMSOL™ for analysing the coupled vibrational system. A 2D FE model was built under the plane stress condition in the solid mechanics interface. Similar numerical analyses had also been performed on other ABH featured structures [26,31]. The local dynamic characteristics of the ABH features were verified to be well captured by using the present FE meshing. The convergence of the present simulation can be conducted in a way similar to [26]. The boundary conditions of the host beam were set to be clamped-clamped. The damping layer and the connector were meshed with quadrilateral elements whilst other parts being meshed using triangular elements. The small connector

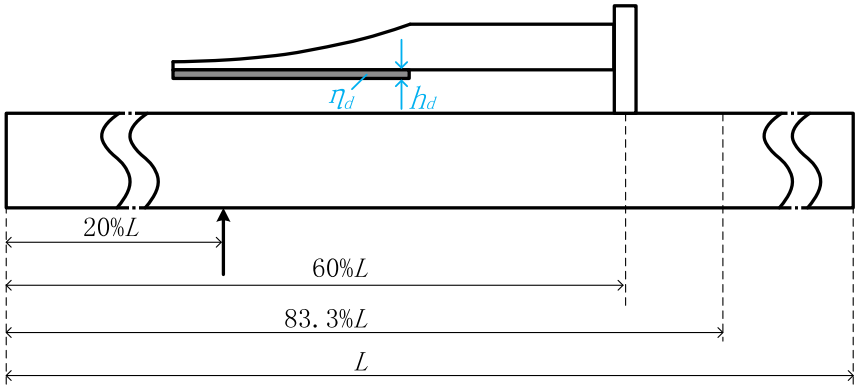

Fig. 2. Schematics of the host beam with an ABH-RBD.

Table 1
Material parameters used in the simulation.

	Aluminum	Damping Layer
Young's modulus	70 GPa	30 MPa
Density	2700 kg/m^3	980 kg/m^3
Poisson's Ratio	0.3	0.499
Loss factor	0.1%	0.9

was set to be a rigid domain. A transverse point excitation was imposed at 20%·L of the host beam. Cross point responses were calculated at 83.3%·L of the host beam from the left end.

3. Vibration suppression phenomena and control mechanisms

Effects of the proposed ABH-RBD are first demonstrated through numerical simulations. The driving and cross point mobility of the host beam are computed for evaluating the control performance of the proposed ABH-RBD and the dynamic characteristics of the combined vibratory system. It can be seen from Fig. 3 that both the driving (Fig. 3(a)) and cross (Fig. 3(b)) point mobility curves of the primary host beam without the ABH-RBD show complex dynamics with multiple resonant peaks within a broad frequency range. With the deployment of the ABH-RBD, most of resonant peaks are suppressed substantially except for some specific resonances. Similar reductions are also observed at other receiver points (not shown here). The ABH-featured add-on device provides effective vibration suppressions of the host beam, and this is achieved without particular tuning of the ABH-RBD parameters. To further demonstrate the generic nature of the observed phenomena, the dimension of the primary beam used above is changed to a longer ($L = 500$ mm) and thinner one, but with the same total weight as the previous one. Naturally, the host structure becomes more flexible with increasing dynamic complexities, as evidenced by more resonant peaks in the same selected frequency range, shown in Fig. 4. As shown in Fig. 4, using the same ABH-featured device on this different beam also leads to a significant reduction in the structural vibration level over the entire frequency range, similar to the previous case. Nevertheless, Fig. 4 shows that no significant and systematic reductions can be obtained at the very low frequency range. This is understandable since systematic ABH effects can only be expected above a certain frequency when local modes within the ABH taper appear. Nevertheless, the proposed ABH-RBD is found to be effective for suppressing the vibrational responses of different host beams using the same ABH-RBD without a particular parameter tuning. Therefore, the broadband peak reduction generated by the add-on structural element with ABH features is shown to be a general phenomenon and the ABH-RBD shows certain robustness for accommodating structural changes in the primary structure.

In order to understand the underlying mechanisms behind the vibration suppression phenomena, analyses are conducted for some typical peaks using the driving point mobility curve in Fig. 3(a). Some typical resonant peaks before the deployment of the ABH-RBD, to be analyzed hereafter, are labeled and identified by dash circles in this figure. These peaks are first

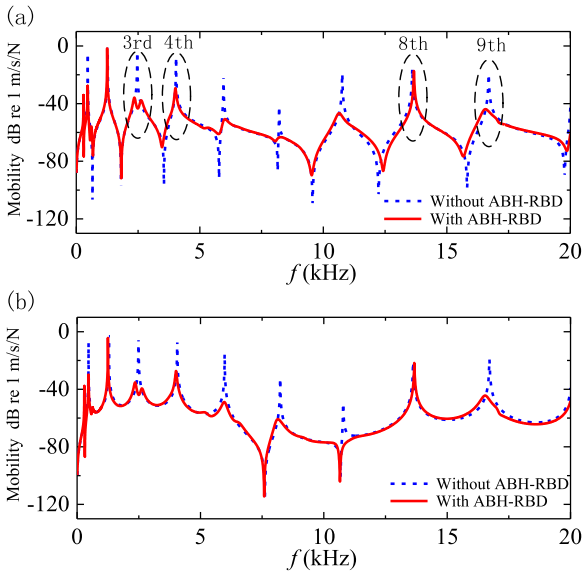

Fig. 3. Comparisons of the (a) driving and (b) cross point mobility of the primary host beam with and without ABH-RBD.

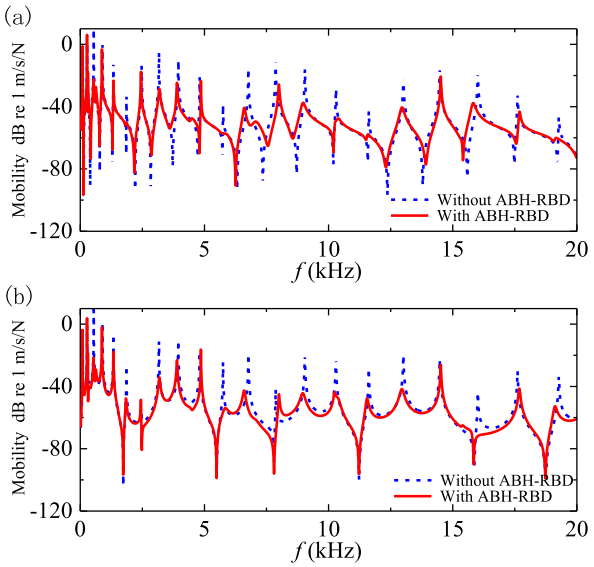

Fig. 4. Comparisons of the (a) driving and (b) cross point mobility of the second host beam with and without ABH-RBD.

classified into different categories based on the way they are affected by the ABH-RBD, whose characteristics are scrutinized at a later stage.

The first group is exemplified by the 3rd resonant peak, marked in Fig. 3(a). It can be seen that the ABH-RBD reduces its vibration amplitude by splitting the peak into two, similar to a conventional DVA. The 4th resonant peak represents another typical category for which the original resonance peak is reduced without being split. For the third category, *i.e.* the 9th one at

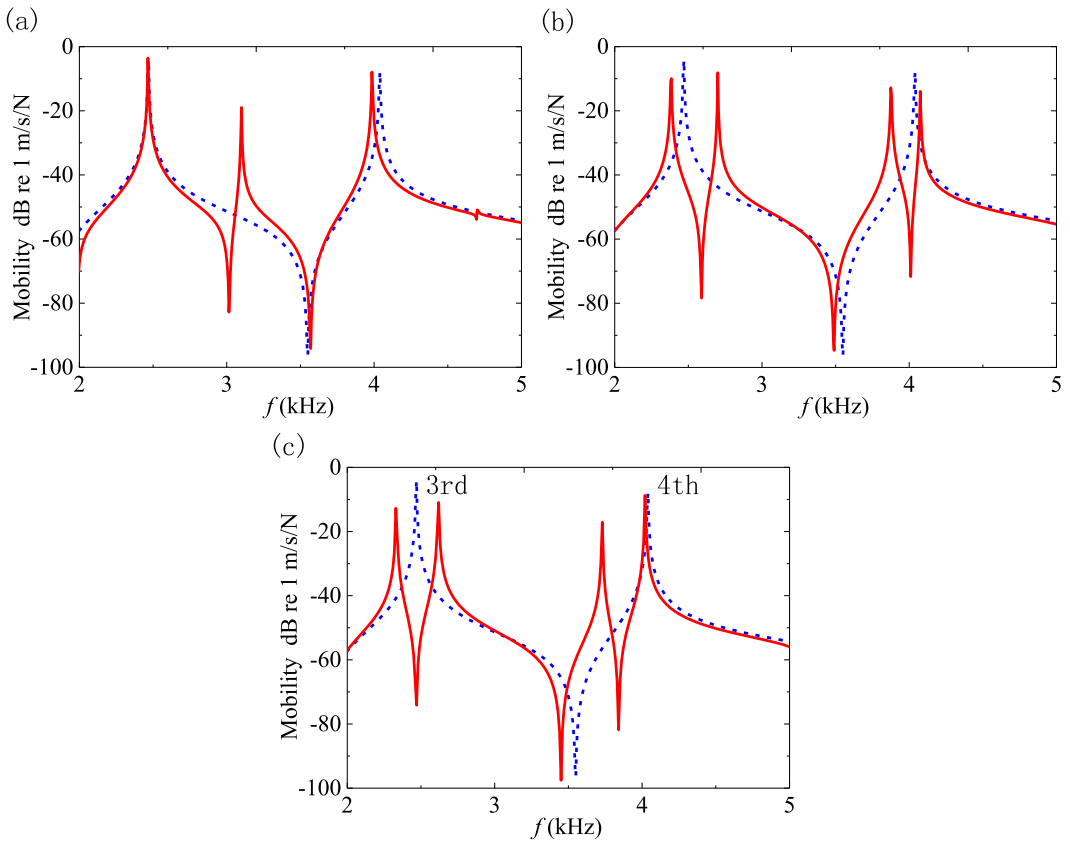

Fig. 5. Driving point mobility of the combined vibratory system with undamped coating layers ($\eta_d = 0$) having different thicknesses: (a) $h_d = 0$mm, (b) $h_d = 0.5$mm and (c) $h_d = 1$mm (solid line '━'); driving point mobility of the primary host beam without any attachment is given as a reference (dash line '┅').

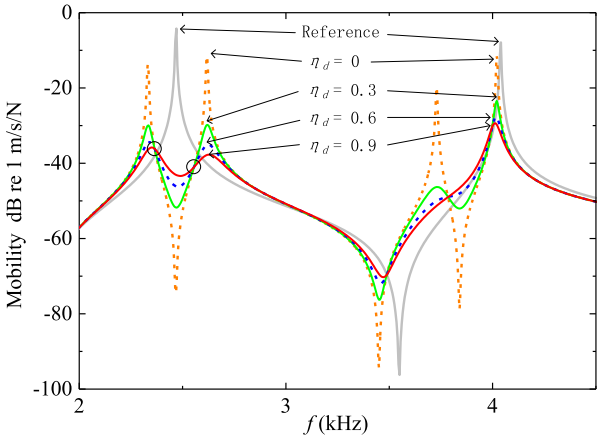

Fig. 6. Driving point mobility of the combined vibratory system with absorbing coating layers with a constant thickness ($h_d = 1$mm) but different loss factors (η_d); the reference is the driving point mobility of the primary host beam without ABH-RBD.

a higher frequency, the original resonance peak seems to be smoothed, shifted without obvious splitting. Meanwhile, the ABH-RBD has little effects on some resonance peaks, exemplified by the 8th resonance frequency.

In order to explore the underlying physics, these different types of peak reductions are scrutinized. By strategically varying the properties of the ABH-RBD, the ABH-induced DVA effect (mainly due to the interaction) and WGA effect (mainly due to the wave trapping and absorption) can be separated. Typical control effects are analyzed through investigating the driving point mobility of the combined vibratory system, first over the frequency band (2–5 kHz) containing the 3rd and 4th resonant peaks and then over the one (13–18 kHz) including the 8th and 9th peaks. The driving point mobility of the primary host beam without ABH-RBD is also provided as a reference.

To single out the effect of structural interaction, the loss factor η_d (refer to Fig. 2) of the coating materials over the tapered portion of the ABH-RBD is first set to zero to eliminate the energy dissipation effect. The dynamics of the ABH-RBD can then be varied by changing the thickness of the undamped coating layer (h_d in Fig. 2). It can be seen from Fig. 5 that with the increase of h_d, the additional peak caused by the ABH-RBD is gradually shifted to the low frequencies and approaches the 3rd resonant peak due to the mass loading effect. Reaching $h_d = 1$mm (same as the one adopted in Fig. 3), the frequency matching condition is satisfied so that strong interactions between the ABH-RBD and the host beam take place around the 3rd original resonance. This is typical of a conventional DVA, resulted from the frequency matching between the DVA and the host structure as well as the strong coupling between both. This peak reduction can be categorized as “interaction-dominated”. It is relevant to note that the undamped ABH-RBD system has little influence on the position of 4th resonance as $h_d = 1$mm.

The damping of the coating layers is then taken into considerations in Fig. 6. Keeping $h_d = 1$ mm, the loss factor of the damping layer (η_d) is varied. An increase in the material damping is expected to enhance the ABH effect [23] to generate more significant energy extractions and dissipations from the host structure. Focusing again on the 3rd and 4th peak frequency range in Fig. 6(a), it can be seen that the 4th peak are gradually reduced when material damping increases, without splitting.

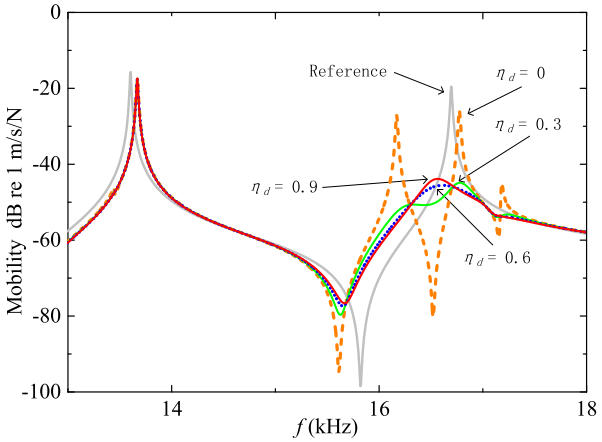

Fig. 7. Driving point mobility of the combined vibratory system with absorbing coating layers with a constant thickness ($h_d = 1$mm) but different loss factors (η_d); the reference is the driving point mobility of the primary host beam without ABH-RBD.

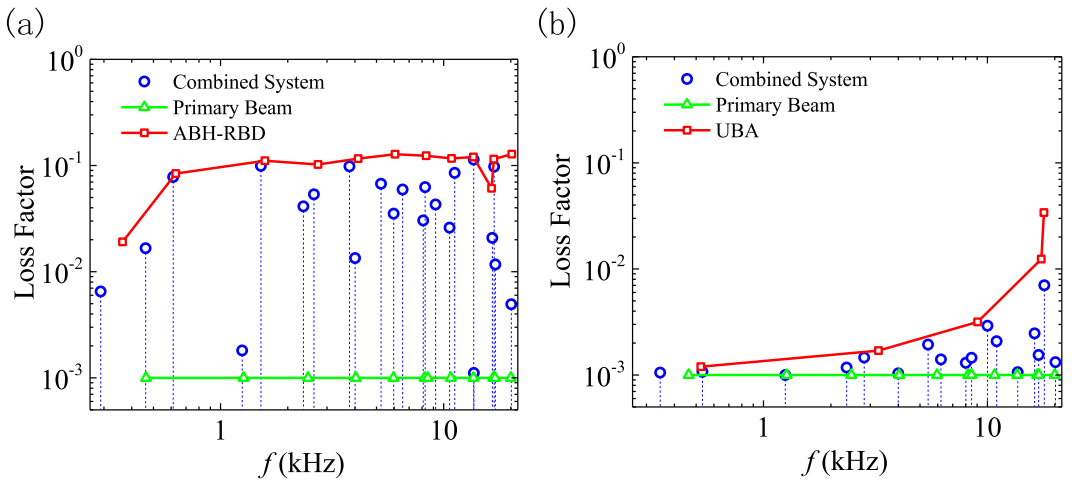

Fig. 8. Loss factors of different system components: primary beam alone, ABH-RBD or uniform beam damper (UBA) alone (with clamped-free ends) and the combined system. (a) ABH-RBD; (b) UBA.

This is the typical phenomenon generated by the damping increase in the overall system due to the waveguide absorber effect of the ABH-RDB. This peak reduction is therefore categorized as "damping-dominated". It is also relevant to re-examine the changes of the 3rd peak (interaction-dominated) due to changes in the system damping. Typical of conventional DVAs, the response curves with different η_d intersect around two fixed points, well documented as the fixed point theory in the literature [1,4]. Obviously, a lower damping would better promote structural interactions, producing more significant narrow-band vibration reductions. An increased damping, however, helps widen the reduction band at the expenses of sacrificing the reduction level. This is also consistent with previous analyses based on conventional DVAs [15].

Adopting the same methodology, changes in another typical peak (identified as the 9th peak in Fig. 3(a)) are examined in Fig. 7 through varying the loss factor (η_d) of the coating material. The peak splitting phenomenon can be seen when η_d is low, suggesting an interaction-dominated feature. When η_d increases, however, the overall system damping quickly increases, leading to an obvious smoothing of the peak due to the imposing damping effect. This happens despite of a relatively small amount of damping material used in the taper of the ABH-RBD. Higher damping level does not necessarily bring about better control performance, which is consistent with the fixed-point theory of conventional DVAs [4]. This type of peak reduction, which seems to occur more frequently in the higher frequency range, is categorized as a combination of the interaction- and damping-dominated phenomenon.

The aforementioned various types of vibration peak reductions are tied with the specific ABH features of the ABH-RBD. To better understand this, Fig. 8(a) shows the loss factors of different components in the system and that of the combined system, using the standard configuration of Fig. 3. For comparisons, same analysis is carried out in Fig. 8(b) for a uniform beam absorber, denoted as UBA. The UBA has the same total weight and thickness (the uniform portion) and the same damping treatment as the ABH-RBD. A few important observations can be made. First, compared with its uniform counterpart (UBA in Fig. 8(b)), the ABH-RBD exhibits much richer dynamics in terms of the number of modes or natural frequencies. This would increase the chance of creating frequency matching to create effective interactions between the ABH-RBD and the primary beam. In fact, when comparing the square dots (absorber modes) with the triangle ones (primary structural modes) in both figures, Fig. 8(a) with the ABH-RBD does produce more matched pairs as compared with Fig. 8(b). Secondly, with the same amount of damping materials used in both cases, the inherent damping of the ABH-RBD well exceeds its uniform counterpart (UBA), due to the superior energy trapping capability of the ABH taper. As a result, the increase in the overall system loss factors is also significantly higher when using ABH-RBD. In the higher frequency range, the broadband ABH absorption effects become more dominant [32,36], which explains the combined interaction- and damping-dominated phenomenon, exemplified by the 9th peak discussed before. This also explains why substantial vibration suppressions can be achieved in the high frequency range with a relatively low damping level of the coating materials (Fig. 7). Therefore, the remarkable vibration suppression capability of the proposed ABH-RBD is indeed attributed to the ABH-specific enrichment of the system dynamics and the broadband damping enhancement in the ABH taper.

To further confirm the superiority of the ABH-RBD, the uniform beam absorber (UBA) used above is added to the primary beam at the same location as before (Fig. 3). The same amount of damping layer is applied from the extended free end of the UBA. It can be seen from Fig. 9 that, although the use of the UBA indeed changes the system dynamics, evidenced by the shift of some resonant peaks alongside the creations of new ones, these peak reductions, albeit noticeable at some frequencies, are marginal compared with Fig. 3(a). This is due to the limited wave-trapping and energy dissipating capacity of the UBA. Therefore, ABH-specific features are vital and essential for the generated broadband vibration control effects.

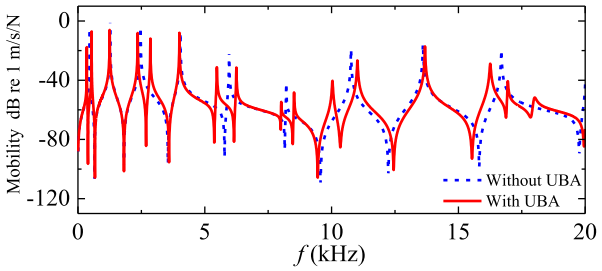

Fig. 9. Comparisons of the driving point mobility of the initial host beam with and without the UBA.

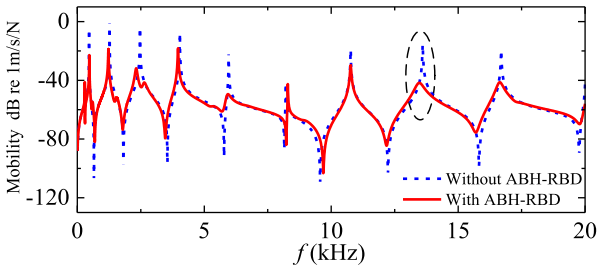

Fig. 10. Driving point mobility of the combined vibratory system with and without an ABH-RBD attached at 80%·L of the primary host beam.

It is relevant to note that ABH-RBD seems to be ineffective for some resonance peaks such as the 8th resonant peak shown in Fig. 3(a). Analyses show that this is due to the attachment location of the ABH-RBD on the primary beam, which, at this particular frequency, generates no energy transfer from the primary beam to the ABH-RBD. The dependence of the vibration control performance of any auxiliary vibration control devices on the attachment position is well known and well documented in the literature [15,19,37]. In the present case, by moving the attachment location of the ABH-RBD to another arbitrarily chosen point, say 80%·L, it can be seen that the 8th resonant peak (circled in Fig. 10) can now be successfully suppressed. This also implies that multiple ABH-RBDs could be used to avoid this situation, and to increases the vibration reductions at the same time.

4. Experimental results

Experiments were conducted to provide a qualitative verification of the predicted broadband vibration suppression phenomena and the corresponding typical vibration control effects.

An ABH-RBD, shown in Fig. 11, was manufactured by the electro discharge machining (EDM) method. Its total length is 120 mm with a width of 19 mm. The tapered portion has the same length (60 mm) as the uniform portion and the thickness varies from 3 mm to 0.2 mm according to the quadratic power-law function ($h(x) = \varepsilon x^2 + h_0$). The ABH-RBD was mounted to a host beam ($500 \times 5 \times 20$mm) through a cuboid connector ($5 \times 4 \times 19$mm) using a super glue. Both the host beam and the ABH-RBD were made of stainless steel. A multi-layered 3M™ F9473PC adhesive tape with a total thickness of 2.08 mm was coated over the surface of the tapered portion of the ABH-RBD. To further increase the energy dissipation capacities of the soft damping material, a liner made of polycoated Kraft is bounded on the outside surface of the damping tape. Similar sandwich damping treatments have also been used in some other experimental studies on ABH [38,39]. The added weight of the ABH-RBD is 10.2% that of the primary beam.

The primary beam was mounted on a rigid metallic frame with its other end free, mimicking a clamped-free boundary conditions. The attachment position of the ABH-RBD was 10%·L from the free end of the host beam. A periodic chirp excitation was used to excite the primary structure at 60%·L from the free end using an electromagnetic shaker. The input force signal was measured by a force transducer (B&K 8203) and amplified by a charge amplifier (B&K 2635). A Polytec™ laser scanning vibrometer (PSV 400) was used to measure the dynamic responses of the host beam. In addition to the driving point mobility, cross point mobility was also measured at 30%·L of the host beam from the free end.

The measured driving and cross point mobility curves of the host beam with and without ABH-RBD are compared in Fig. 12. It can be seen that, when the ABH-RBD is mounted, the resonant peaks of the primary system are effectively suppressed over the broad frequency range of interest, except for some particular frequencies, which is consistent with the general vibration reduction phenomena predicted by numerical simulations. In particular, typical resonance peak variations, as analyzed above, can also be seen. For example, the interaction-dominated peak reduction with the split-up phenomenon can be clearly seen, as marked by the first circle in Fig. 12(a), as well as some other peaks. Note that this happened without particular tuning of the ABH-RBD. The rich dynamics of the ABH-RBD actually increases the chance for this to take place.

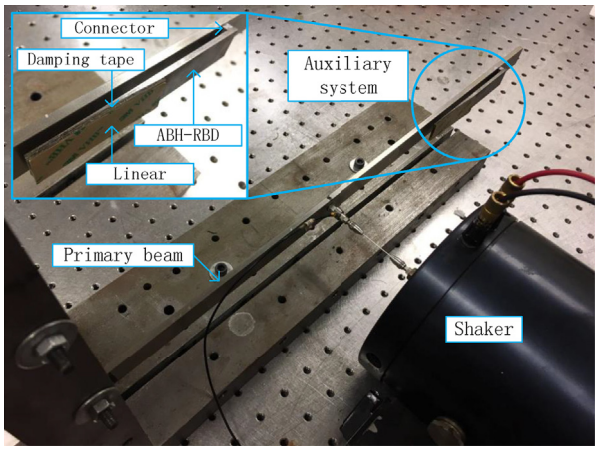

Fig. 11. Experimental set-up.

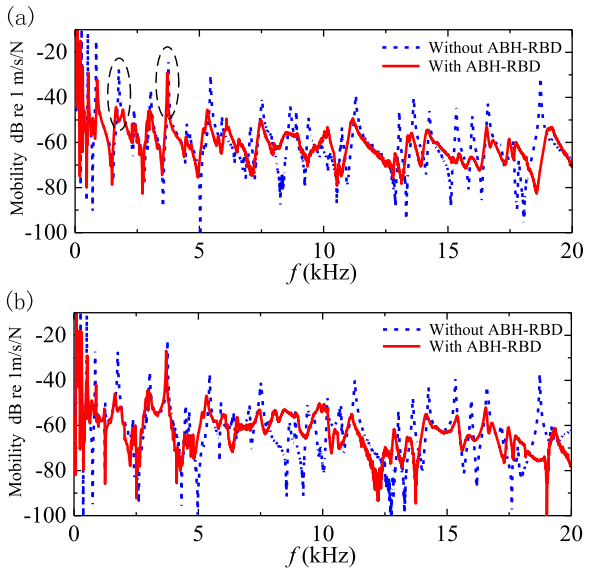

Fig. 12. Comparisons of the measured (a) driving and (b) cross point mobility of the primary host beam with and without ABH-RBD.

Meanwhile, we do observe some peaks, *i.e.* the second circled peak, on which, the ABH-RBD seems to be in-effective, due to the attachment location. Most of peaks, however, are reduced around the original resonance frequency owing to either ABH-induced broadband damping enhancement, or the combined interaction and damping effect at higher frequencies. As a whole, the significant vibration reduction effect as well as different types of peak reductions (interaction-dominated, damping-dominated, their combination and the location-dependent loss of effectiveness) are all confirmed by experiments.

The ABH-RBD was then replaced by a uniform beam absorber (UBA) with the same total weight, the same thickness (uniform portion) and the same damping treatment. It can be seen from Fig. 13 that the dynamics of the primary host beam are affected, as evidenced by alterations on the mobility curves. Although the added damping allows some peak reductions at some particular frequencies, the overall reduction level, however, is relatively low as compared with that provided by the ABH-RBD.

5. Conclusions

In this paper, we propose a new type of vibration control device for the broadband vibration suppressions of vibrating structures. By capitalizing on the Acoustic Black Hole (ABH) phenomena, the proposed ABH-featured Resonant Beam Damper (ABH-RBD) embraces the principles of both dynamic vibration absorbers and waveguide absorbers. With a relatively simple

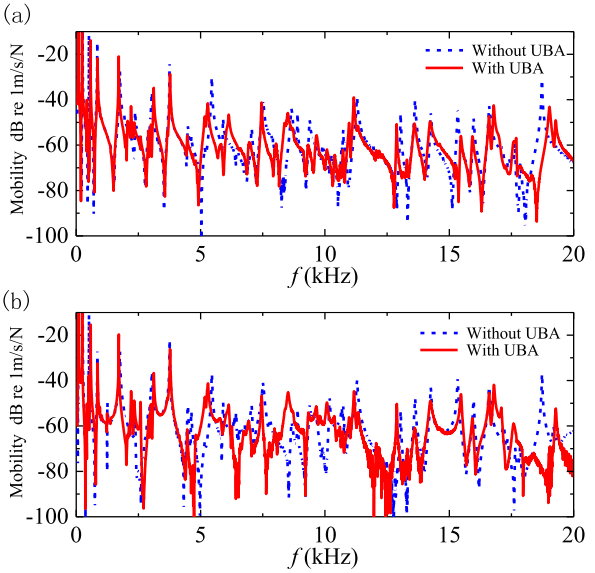

Fig. 13. Comparisons of the measured (a) driving and (b) cross point mobility of the host beam with and without UBA.

and easily achievable configuration, the ABH-featured add-on device does not require complex parameter tuning in the design process, showing certain robustness for accommodating structural variations in the primary structure.

Using a beam as a benchmark structure, the effectiveness of the proposed ABH-RBD, as well as the underlying mechanisms, are demonstrated through numerical simulations and confirmed through experimental measurements. It is shown that, the ABH-specific features of the device, in terms of its enriched dynamics and enhanced damping, maximizes the structural interaction as well as energy extraction and dissipation from the host structure. As a result, broadband vibration reductions can be achieved, by using the same ABH-RBD on different primary systems, provided the location of the attachment is properly chosen.

Analyses reveal three typical vibration reduction mechanisms, dominated by interaction, damping and their combination, respectively. Interaction-dominated peak reduction is similar to conventional dynamic absorber. However, the proposed ABH-RBD is shown to exhibit much richer dynamics in terms of number of modes or natural frequencies than conventional structural elements. This increases the chance of creating better frequency matching with the primary structure and more effective interactions. The damping-dominated peak reductions are due to the remarkable energy trapping capability of the ABH taper. This allows the use of a small amount of damping materials to achieve a significant increase in the overall damping of the system. In the high frequency range, when the broadband ABH absorptions are more dominated, the enhanced damping is combined with the interaction effect, thus resulting in a significant vibration reduction, manifested by a smoothing and shifting of the resonance peaks of the primary structure.

As a final remark, it should be mentioned that the proposed ABH-RBD is not limited to one dimensional case. The device can also be materialized through different engineering designs. For example, the ABH-RBD can be designed to a spiral shape to make it more compact in size [28]. Meanwhile, multiple ABH-RBDs can be used to increase the control performance by avoiding the location-dependent loss of effectiveness when only one ABH-RBD is used.

In conclusion, the proposed ABH-RBD has been shown to be a good candidate for the suppressions of broadband multi-resonances of a vibrating structure, also extendable to other applications such as noise reductions and energy harvesting.

Acknowledgements

The authors would like to acknowledge the Research Grant Council of the Hong Kong SAR (PolyU 152009/15E and PolyU 152026/14E) and National Science Foundation of China (No. 11532006) for financial support.

References

[1] D.J. Mead, Passive Vibration Control, John Wiley & Sons, New York, 1998.
[2] J.B. Hunt, Dynamic Vibration Absorbers, Mechanical Engineering Publications, London, 1979.
[3] D.J. Inman, Engineering Vibration, Prentice Hall, New Jersey, 2001.
[4] J.P. Den Hartog, Mechanical Vibrations, Courier Corporation, New York, 1956.
[5] B.G. Korenev, L.M. Reznikov, Dynamic Vibration Absorbers: Theory and Technical Applications, John Wiley & Sons, New York, 1993.
[6] A.D. Nashif, D.I.G. Jones, J.P. Henderson, Vibration Damping, John Wiley & Sons, New York, 1985.

[7] D.I.G. Jones, A.D. Nashif, H. Stargardter, Vibrating beam dampers for reducing vibrations in gas turbine blades, Journal of Engineering for Power 97 (1) (1975) 111–116.
[8] M. Brennan, Characteristics of a wideband vibration neutralizer, Noise Control Eng. J. 45 (5) (1997) 201–207.
[9] L. Zuo, S.A. Nayfeh, Minimax optimization of multi-degree-of-freedom tuned-mass dampers, J. Sound Vib. 272 (3) (2004) 893–908.
[10] H. Yamaguchi, Vibrations of a beam with an absorber consisting of a viscoelastic beam and a spring-viscous damper, J. Sound Vib. 103 (3) (1985) 417–425.
[11] D. Manikanahally, M. Crocker, Vibration absorbers for hysterically damped mass-loaded beams, J. Vib. Acoust. 113 (1) (1991) 116–122.
[12] J. Snowdon, Vibration of cantilever beams to which dynamic absorbers are attached, J. Acoust. Soc. Am. 39 (5A) (1966) 878–886.
[13] D.A. Rade, V. Steffen, Optimisation of dynamic vibration absorbers over a frequency band, Mech. Syst. Signal Process. 14 (5) (2000) 679–690.
[14] R. Jacquot, Suppression of random vibration in plates using vibration absorbers, J. Sound Vib. 248 (4) (2001) 585–596.
[15] C. Yang, D. Li, L. Cheng, Dynamic vibration absorbers for vibration control within a frequency band, J. Sound Vib. 330 (8) (2011) 1582–1598.
[16] E.E. Ungar, L.G. Kurzweil, Preliminary Evaluation of Waveguide Vibration Absorbers, Bolt Beranek and Newman Inc, Cambridge Ma, 1984.
[17] G.G. Lee, Analytical and Experimental Studies of Beam Waveguide Absorbers for Structural Damping, Naval Postgraduate School, Monterey, California, 1988.
[18] Y. Shin, S. Watson, K. Kim, Passive vibration control scheme using circular viscoelastic waveguide absorbers, J. Pressure Vessel Technol. 115 (3) (1993) 256–261.
[19] S.J. Watson, Experimental Studies of Circular Viscoelastic Waveguide Absorbers for Passive Structural Damping, Naval Postgraduate School, Monterey, California, 1989.
[20] C.M. Pray, S.A. Hambric, T.E. McDevitt, C.B. Burroughs, Characterization of folded beam waveguide absorbers for damping of flexural vibrations in a thick plate, Noise Control Eng. J. 48 (6) (2000) 185–192.
[21] E.E. Ungar, L. Kurzweil, Structural Damping Potential of Waveguide Absorbers, Bolt Beranek and Newman Inc, Cambridge Ma, 1984.
[22] M.A. Mironov, Propagation of a flexural wave in a plate whose thickness decreases smoothly to zero in a finite interval, Sov. Phys. Acoust. 34 (3) (1988) 318–319.
[23] V.V. Krylov, F.J.B.S. Tilman, Acoustic 'black holes' for flexural waves as effective vibration dampers, J. Sound Vib. 274 (3) (2004) 605–619.
[24] V. Denis, A. Pelat, F. Gautier, B. Elie, Modal Overlap Factor of a beam with an acoustic black hole termination, J. Sound Vib. 333 (12) (2014) 2475–2488.
[25] L. Tang, L. Cheng, H. Ji, J. Qiu, Characterization of acoustic black hole effect using a one-dimensional fully-coupled and wavelet-decomposed semi-analytical model, J. Sound Vib. 374 (2016) 172–184.
[26] T. Zhou, L. Tang, H. Ji, J. Qiu, L. Cheng, Dynamic and static properties of double-layered compound acoustic black hole structures, International Journal of Applied Mechanics 9 (05) (2017), 1750074.
[27] L. Tang, L. Cheng, Enhanced Acoustic Black Hole effect in beams with a modified thickness profile and extended platform, J. Sound Vib. 391 (2017) 116–126.
[28] J.Y. Lee, W. Jeon, Vibration damping using a spiral acoustic black hole, J. Acoust. Soc. Am. 141 (3) (2017) 1437–1445.
[29] L. Zhao, S. Conlon, F. Semperlotti, Broadband energy harvesting using acoustic black hole structural tailoring, Smart Mater. Struct. 23 (6) (2014), 065021.
[30] L. Tang, L. Cheng, Broadband locally resonant band gaps in periodic beam structures with embedded acoustic black holes, J. Appl. Phys. 121 (19) (2017), 194901.
[31] L. Tang, L. Cheng, Ultrawide band gaps in beams with double-leaf acoustic black hole indentations, J. Acoust. Soc. Am. 142 (5) (2017) 2802–2807.
[32] S.C. Conlon, J.B. Fahnline, F. Semperlotti, Numerical analysis of the vibroacoustic properties of plates with embedded grids of acoustic black holes, J. Acoust. Soc. Am. 137 (1) (2015) 447–457.
[33] D.J. O'Boy, V.V. Krylov, Damping of flexural vibrations in circular plates with tapered central holes, J. Sound Vib. 33 (10) (2011) 2220–2236.
[34] L. Ma, S. Zhang, L. Cheng, Vibration of a Plate with Power-law-profiled Thickness Variation by Wavelet Decomposed Rayleigh-ritz Method, Inter noise, Hong Kong, China, August 27-30, 2017.
[35] W. Liu, M.S. Ewing, Experimental and analytical estimation of loss factors by the power input method, AIAA J. 45 (2) (2007) 477–484.
[36] P.A. Feurtado, S.C. Conlon, An experimental investigation of acoustic black hole dynamics at low, mid, and high frequencies, J. Vib. Acoust. 138 (6) (2016), 061002–061002.
[37] R.G. Jacquot, Optimal damper location for randomly forced cantilever beams, J. Sound Vib. 269 (3) (2004) 623–632.
[38] D.J. O'Boy, E.P. Bowyer, V.V. Krylov, Point mobility of a cylindrical plate incorporating a tapered hole of power-law profile, J. Acoust. Soc. Am. 129 (6) (2011) 3475.
[39] O. Unruh, C. Blech, H.P. Monner, Numerical and experimental study of sound power reduction performance of acoustic black holes in rectangular plates, SAE International Journal of Passenger Cars-Mechanical Systems 8 (2015–01-2270) (2015) 956–963.